
Article:
Wu, J., Dong, G. and Li, Y. orcid.org/0000-0001-7907-5176 (2019) Parallel chemistry acceleration algorithm with ISAT table-size control in the application of gaseous detonation. Shock Waves, 29 (4). pp. 523-535. ISSN 0938-1287

https://doi.org/10.1007/s00193-018-0880-7

Submitted to Shock Waves

Paper type：Full-length

Parallel chemistry acceleration algorithm with ISAT table size control in the application of gaseous detonation

Jintao Wu[1], Gang Dong[1,*], Yi Li[2]

1. Key Laboratory of Transient Physics, Nanjing University of Science and Technology, Nanjing 210094, Jiangsu, China;
2. School of Mathematics and Statistics, University of Sheffield, Sheffield S3 7RH, U.K.

Abstract In order to improve the computational efficiency of parallel ISAT-based chemistry acceleration algorithm in the computations of transient, chemically reacting flows, a control strategy is proposed to maintain the size of data tables in ISAT computations. This table size control strategy is then combined with the selected parallel algorithm for the application in the numerical simulations of two-dimensionally gaseous detonation wave propagation. Two different control methods namely total table size (M_{tot}) control and single table size (M_{sin}) control are adopted in the novel strategy. The maximum speedup ratios of 4.29 and 5.52 are obtained for the cases with fixed total table size and the cases with fixed single size, respectively, in the computations of $2H_2+O_2$ detonations. Furthermore, two parameters, σ_f and p, are proposed to analyze equilibrium and synchronization among table operations in the parallel ISAT computations with the table size control strategy. It is found that both equilibrium and synchronization among data tables have the obvious influences on the speedup ratio. A parameter p_M for choosing the optimal table sizes (both M_{tot} and M_{sin}) is subsequently proposed and is then verified to be universal either in computations of $2H_2+O_2$

*Corresponding author.
E-mail address: dgvehicle@yahoo.com

detonations or in computations of $C_2H_4+3O_2$ detonations. Lastly, the computational accuracies of selected cases computed by the parallel acceleration algorithm with table size control strategy are examined and to be reliable for both fuels detonations.

Keywords parallel chemistry acceleration algorithm; table size control strategy; equilibrium and synchronization; gaseous detonation.

1. Introduction

In the reacting flow computations with detailed chemical mechanism, the characteristic timescales among chemical species are extremely different from one to another [1]. This leads to the serious stiffness and further causes the expensively computational costs when chemical source term is directly integrated. To remedy this problem, various storage/retrieval methods based on tabulation (e.g. [2-9]) is proposed for accelerating the chemical reaction computations in the simulations of different realistic reacting flows. Among all these methods, an ISAT technique [6] constructs a data table for implementing the operations of chemical reaction data including query, insertion and retrieval. Thus, the time-consuming processes of direct integration in the computations of chemical reactions are replaced by the time-saving table operations. Therefore, the ISAT technique is widely applied in different calculations of chemically reacting flows and examined to be fruitful in both the series computations [10-14] and the parallel computations [15-17].

However, the performance of the ISAT technique is strongly dependent on the specific physical problems. In the computations of steady combustion problems with low Mach number flows, most of data in a table can be successfully retrieved due to the small variation of thermodynamic states in flow field within each time-step, thus the chemistry acceleration of the original ISAT algorithm shows the excellent performance [18-21]. However, for the unsteady combustion problems in compressible flows, some of data may not be successfully retrieved due to the large change of thermodynamic states within one time-step, which leads to a limited acceleration of the original ISAT algorithm. Furthermore, reduction on the retrieval rate of thermodynamic states means that some new data have to be inserted into the table and thus give rise to the excessive growth of table size which may reach the upper limit of computer memory. Consequently, Dong et al. developed a dynamic storage/deletion algorithm [22, 23] based on a reduced ISAT technique to maintain the table size. In this algorithm, two different deletion methods of the data table were proposed and showed the good controlling effect to the table size in the series computations of gaseous detonation problems, without the loss of the computational accuracy.

However, in the parallel computations, there exist multiple tables corresponding to different sub-zones of the computational domain. Intuitively, for all sub-zones, a table should be built in its own sub-zone and the corresponding table operations should be performed locally. This parallel strategy is called as the *purely local processing* (PLP) by Lu et al. [24]. Other parallel strategies and

a so-called adaptive strategy are constantly proposed [24-28] in recent years and have been incorporated into the package named *x2f_mpi* [25]. However, these parallel strategies are mainly applied to the computations of steady combustion process with low Mach number flows. For strongly compressible, unsteady reacting flows, such as gaseous detonations, the introduction of the deletion mechanism in ISAT method increases the complexity of the problems. For example, it is possible that the loads of tabulation operations are different among the tables in their own sub-zones, because the thermodynamic states of different sub-zones are always different. Therefore, growth rate of table size for each table is different from those for other tables. Since the standard of judging the computational acceleration is the wall-clock time, the difference can give rise to the deterioration of synchronization of tabulation operations among the tables and then delay the wall-clock time. For a user who has the computer installation with known total memory and known processor number, it is important to allocate the computational resources into the different tables and then get the optimal table size and the maximum acceleration in the parallel computations. Therefore, it is necessary to develop the new controlling methods of table size to balance the operations among different tables in the parallel chemistry acceleration algorithm based on the reduced ISAT technique with the deletion process.

In this paper, a parallel algorithm for the chemically acceleration named TP/DEP [29] is selected to be combined with the innovative table size control strategy. Unlike the ref. [29] in which only a fixed upper limit of table size for each table is set, we investigate the effects of two controlling factors of table size, namely single table size control and total table size control, on the algorithm performance in the simulations of two-dimensionally gaseous detonation wave propagation in present work. The outline of this paper is as follows. In Sec. 2, the reduced ISAT technique with our new table size control strategy is described and then, a TP/DEP algorithm which constructed by two different types of parallel strategy is introduced. The computational details including the governing equations, the initial physical conditions and the numerical schemes are given in Sec. 3. The computational efficiency and accuracy of the parallel algorithm within different cases of table size control are in Sec. 4, while the equilibrium and synchronization analyses are also given in this section. Lastly, Sec. 5 presents the conclusions.

2. Algorithm Descriptions

2.1. The reduced ISAT method with novel table size control strategy

The basic frame of the ISAT algorithm originally proposed by Pope [6] can be briefly introduced as follows. Considering a compressible system of chemically reacting flows with K species, a thermodynamic state function $\mathbf{\Phi}$ can be expressed as

$$\mathbf{\Phi}=(Y_1,\cdots Y_k,\cdots Y_K,\ T,\ \rho)=(\phi_1,\ \ldots,\ \phi_k,\ \ldots,\ \phi_K,\ \phi_{K+1},\ \phi_{K+2}) \tag{1}$$

here Y_k (k=1, …, K) is the mass fraction of k-th species in the system, T and ρ are the temperature and density of the system, respectively. When chemical reactions occur within one time-step Δt, a change of $\mathbf{\Phi}$, $\mathbf{R}(\mathbf{\Phi})$, can be obtained by the following direct integration (DI) method

$$\mathbf{R}(\mathbf{\Phi})=\mathbf{\Phi}_1-\mathbf{\Phi}_0=\int_{\Delta t}\mathbf{S}\mathrm{d}t \tag{2}$$

here, $\mathbf{\Phi}_0$ and $\mathbf{\Phi}_1$ are the thermodynamic states just before and after the time-step Δt, $\mathbf{S}$ denotes the chemical source term. Usually the Eq. (2) can be performed by using ordinary differential equation (ODE) solver.

Instead of above DI method, the change due to chemical reactions can be approximated by the query/retrieval process to a data table in the original ISAT technique [6]. Consider a thermodynamic vector $\mathbf{\Phi}^q$ that needs to be queried in system, if the vector is close to a known vector $\mathbf{\Phi}^{(j)}$ in the table, its change, $\mathbf{R}(\mathbf{\Phi}^q)$, can be obtained in a linear approximation form by a Taylor series expansion based on $\mathbf{\Phi}^{(j)}$ and $\mathbf{R}(\mathbf{\Phi}^{(j)})$

$$\mathbf{R}(\mathbf{\Phi}^q)=\mathbf{R}(\mathbf{\Phi}^{(j)})+\frac{\partial R(\mathbf{\Phi}^{(j)})}{\partial\mathbf{\Phi}^{(j)}}\Delta\mathbf{\Phi}+O(|\Delta\mathbf{\Phi}|^2) \tag{3}$$

here, $\Delta\mathbf{\Phi}=\mathbf{\Phi}^q-\mathbf{\Phi}^{(j)}$. Eq. (3) produces the computation and storage of term $\partial\mathbf{R}(\mathbf{\Phi}^{(j)})/\partial(\mathbf{\Phi}^{(j)})$ that is a mapping gradient matrix $\mathbf{A}$. The manipulation of $\mathbf{A}$ yields an ellipsoid of accuracy (EOA) with a given error tolerance $\varepsilon_{\mathrm{tol}}$[6, 19]. If the queried vector $\mathbf{\Phi}^q$ falls into the range of EOA of $\mathbf{\Phi}^{(j)}$, $\mathbf{R}(\mathbf{\Phi}^q)$ can be retrieved as a linear approximation of $\mathbf{R}(\mathbf{\Phi}^{(j)})$ via Eq. (3). The query/retrieval process in the data table greatly saves the computational cost relative to the DI method (Eq. 2) and thus shows the chemical acceleration effect. Moreover, well-controlled $\varepsilon_{\mathrm{tol}}$ can ensure the satisfactory accuracy for computations of reacting flows.

Unlike the original ISAT method, we adopted a constant (zero-order) approximation to obtain $\mathrm{R}(\mathbf{\Phi}^q)$, which is expressed as

$$\mathbf{R}(\mathbf{\Phi}^q)=\mathbf{R}(\mathbf{\Phi}^{(j)})+O(|\Delta\mathbf{\Phi}|) \tag{4}$$

Thus, a range of error $\mathbf{\Phi}^{(j)}$ should be artificially constructed to meet the accuracy of constant approximation. In our reduced ISAT method [22], two error arrays are set as the range of error for

a tabulation vector $\mathbf{\Phi}^{(j)}$

$$e^{\pm}(\mathbf{\Phi}^{(j)}) = \{e_1^{\pm}(\phi^{(j)}), \cdots, e_k^{\pm}(\phi^{(j)}), \cdots, e_{K+2}^{\pm}(\phi^{(j)})\} \tag{5}$$

The arrays actually constitute a hyper-rectangle of accuracy (ROA) for $\mathbf{\Phi}^{(j)}$, in which the computations and storages of mapping matrix **A** in Eq. (3) are avoided and thus further reduce the CPU time on reaction mapping. Besides the constant approximation, a nodal deletion strategy [23] is also introduced to control the table size during the implementation the reduced ISAT. Thus, the procedure of our reduced ISAT can be described as follows:

(i) An empty data table is initially built in the computer memory. The first thermodynamic state vector on a grid of flow field has to be integrated via Eq. (2), as a result, the state vector, its change and corresponding error arrays are stored as a node "*j*" in the table, that is, $\mathbf{\Phi}^{(j)}$, $\mathbf{R}(\mathbf{\Phi}^{(j)})$ and $e^{\pm}(\mathbf{\Phi}^{(j)})$.

(ii) For a queried state vector $\mathbf{\Phi}^{q}$, the $\mathbf{\Phi}^{(j)}$ in the table is firstly searched and compared with $\mathbf{\Phi}^{q}$. If all elements in $\mathbf{\Phi}^{q}$ satisfies

$$\phi_k^{(j)} - e_k^{-} < \phi_k^{q} < \phi_k^{(j)} + e_k^{+} \quad (k=1,\ \ldots,\ K,\ K+1,\ K+2) \tag{6}$$

for a given tabulation vector $\mathbf{\Phi}^{(j)}$, the constant approximation in Eq. (4) is performed and the data of $\mathbf{\Phi}^{(j)}$ and $\mathbf{R}(\mathbf{\Phi}^{(j)})$ are retrieved as values of the queried vector and its change, $\mathbf{\Phi}^{q}$ and $\mathbf{R}(\mathbf{\Phi}^{q})$. In this case, the query is successful.

(iii) If Eq. (6) is not satisfied, Eq. (2) is employed to obtain $\mathrm{R}(\mathbf{\Phi}^{q})$ for $\mathbf{\Phi}^{q}$. Simultaneously, a node with tabulation vector $\mathbf{\Phi}^{(n)}$ that is closest to the $\mathbf{\Phi}^{q}$ along the querying path in the table is recorded. Comparing the $\mathbf{R}(\mathbf{\Phi}^{q})$ with $\mathbf{R}(\mathbf{\Phi}^{(n)})$ in that node with a given error tolerance $\varepsilon_{\mathrm{tol}}$, if

$$\max \frac{|R(\phi_k^{q}) - R(\phi_k^{(n)})|}{|\phi_k^{q}|} \le \varepsilon_{\mathrm{tol}} \tag{7}$$

for any component *k*, *k*-th component of $e^{\pm}(\mathbf{\Phi}^{(n)})$ will be enlarged until all components of the $\mathbf{\Phi}^{q}$ are included in the range of the ROA of $\mathbf{\Phi}^{(n)}$. If Eq. (7) is not satisfied, a new node including $\mathbf{\Phi}^{q}$, $\mathrm{R}(\mathbf{\Phi}^{q})$ and corresponding $e^{\pm}(\mathbf{\Phi}^{q})$ are inserted (stored) in the table. Thus, the size of the data table grows and a new query repeats again from (ii) to (iii).

It should be note that the enlargement of the ROA is important in the reduced ISAT method. Although Eq. (7) does not ensure the retrieval of queried vector at current query, it can increase the retrieval probability of the vector at the next query within enlarged range of ROA. Assuming a vector $\mathbf{\Phi}^{q'}$ in the next query (after the chemical mapping) is satisfies the Eq. (6) for the record node *n* with the enlarged ROA, this means

$$\mathbf{\Phi}^{q'} = \mathbf{\Phi}^{(n)} + \mathbf{R}(\mathbf{\Phi}^{q}) \tag{8}$$

In addition, for recorded node n, we have vector $\mathbf{\Phi}^{n'}$ after the chemical mapping

$$\mathbf{\Phi}^{n'} = \mathbf{\Phi}^{(n)} + \mathbf{R}(\mathbf{\Phi}^{(n)}) \tag{9}$$

Thus, combining Eqs. (8) and (9) for all components of the vectors with Eq. (7) yields

$$\frac{|\phi_k^{q'} - \phi_k^{(n')}|}{|\phi_k^{q'}|} = \varepsilon_{\text{tol}} \quad (k=1,\ \ldots,\ K,\ K+1,\ K+2) \tag{10}$$

on the boundary of enlarged ROA. Obviously, ε_{tol} in Eq. (10) actually means the relative error between $\phi_k^{q'}$ and $\phi_k^{(n')}$ after the chemical mapping.

The error arrays in Eq. (5) can be defined as

$$\mathrm{e}_k^{\pm}(\phi^{(j)}) = \pm(\varepsilon_{\mathrm{r}}\phi_k^{(j)} + \varepsilon_{\mathrm{a}}) \tag{11}$$

Here, the relative error, ε_{r}, and the absolute error, ε_{a}, are set to be 1×10^{-3} and 1×10^{-8} respectively in present study. The value of ε_{r} represents the retrieval accuracy of queried vector only if Eq. (5) is satisfied. Otherwise the ROA will be enlarged so that the ε_{tol} represents the retrieval accuracy in the subsequent queries based on Eq. (10). Usually the ε_{r} should be no more than ε_{tol}. The smaller ε_{r} can leads to the more enlarged events whose retrieval accuracy is finally decided by ε_{tol}. If $\varepsilon_{\mathrm{r}}>\varepsilon_{\text{tol}}$, the enlarged events will seldom occur and retrieval accuracy is mainly determined by ε_{r}. In present study, we set $\varepsilon_{\text{tol}}=1\times10^{-3}$. The same values of ε_{tol} and ε_{r} ensure that the retrieval accuracy in present study is 1×10^{-3} regardless of enlargement of ROA or not. Note that ε_{tol} and ε_{r} are different because the former is global while the latter is local. The ε_{tol} finally plays an important role in determining the retrieval accuracy. The value of ε_{tol} (1×10^{-3}) set in this study has been examined to be accurate in the problem of gaseous detonation wave propagation for both the series computation [22, 23] and the parallel computation [29]. On the other hand, ε_{a} can take a sufficient small quantity to maintain the non-negativity of $\mathbf{\Phi}$. The 1×10^{-8} of ε_{a} in present study implies that the non-negativity of the $\phi_k^{(j)}$ requires $\phi_k^{(j)} \geq \varepsilon_{\mathrm{a}}/(1-\varepsilon_{\mathrm{r}}) \approx 1.001\times10^{-8}$, thus, we set $\phi_k^{(j)} = 1.005\times10^{-8}$ if $\phi_k^{(j)}$ is less than this value so that the thermodynamic state in the system is positive.

(iv) If large amount of new nodes that do not satisfy Eq. (7) have to be inserted into the table, they can lead to a rapid growth of table, which makes the table size reach the upper limit of computer memory and therefore interrupts the computations. This is particularly true for the computations of transient, compressible, reacting flows, in which the change of thermo-chemical states is so large within one time-step that some stored nodes (data) cannot be retrieved frequently. To avoid this, a

table size control method with two controlling factors, namely single table size (M_{sin}) control and total table size (M_{tot}) control, is proposed in present study during the parallel ISAT computations. For the M_{sin} control, a nodal deletion operation [23] for the single table is activated when the size of this table reaches M_{sin}; while for the M_{tot} control, the nodal deletion operation is performed for each table only if the total size of all tables reaches M_{tot}. In addition, we further improve the detail of nodal deletion mechanism proposed in ref. [23], that is, all nodes that have ever been retrieved during the whole computations are reserved, and the rest of the nodes are deleted. This is different from that in ref. [23] that only nodes after last deletion operation are reserved. Although the accumulation of data nodes will certainly occupy a part of space of table, these reused data can increase the retrieval rate of nodes.

In the reduced ISAT technique with the new table size control strategy, a data structure with balanced binary tree (BBT) is used to construct the data table [22, 23]. The typical table operations in this study include query, retrieval, insertion, balance, enlargement and deletion of nodes in the table, here the balance operation is used to adjust the depth of the two sub-trees of every node so that the depth of both sub-trees is never different by more than one in BBT. Of all these operations, query, insertion, balance and deletion involve in the traversal of BBT. The first three are executed by a global traversal process, while the last one is achieved by a non-recursive traversal process.

2.2. The parallel ISAT algorithm to the gaseous detonation simulation

For parallel simulations of the two-dimensional gaseous detonation simulations in present study, a chemistry acceleration algorithm named TP/DEP [29] is selected and used. This algorithm consists of two parallel strategies namely *transposed processing* (TP) and *data exchange processing* (DEP), as shown in Fig. 1. For the TP strategy in Fig. 1(a), the sub-zones (S_1-S_n) of the computational domain with same rectangle shape are distributed along the direction of detonation wave propagation, while the data tables (T_1-T_n) are built into the sub-zones S_1-S_n in the corresponding transposed location. Thus, each table handles the data collected from the data blocks of the same position in different sub-zones, in according to the reduced IAST method with nodal deletion described in Sec. 2.1. When the detonation wave (DW in Fig. 1) moves upward along the direction that is perpendicular to the boundaries of between the sub-zones, the corresponding data blocks from these sub-zones can be reorganized into the transposed tables which have the similar distributions of thermodynamic states among them. Therefore, it is expected that each table has the

similar operation load for the purpose of table operation equilibrium among different tables.

The ISAT tables are very complicated to handle in an efficiently parallel manner because the specific table operation within one time-step is still different among tables, although a TP strategy is employed. Thus, a DEP strategy that further improves the equilibrium of table operations through the data exchanges among the tables is proposed [29] besides the TP strategy, as illustrated in Fig. 1(b). In this strategy, we first record the accumulated CPU times (wall-clock times) cost by table operations for each table before current time-step. Then, a half of data in the table with maximum wall-clock time (T_{max} in Fig. 1b) is exchanged with that in the table with minimum wall-clock time (T_{min} in Fig. 1b) through the functions of MPI_SEND and MPI_RECV in Message Passing Interface (MPI) technique. Similarly, such exchange process is executed between the table with second-maximum wall-clock time and the table with second-minimum wall-clock time simultaneously, and so on. Once all table operations are completed within current time-step, the exchanged data are transmitted back to their own tables. Lastly, the accumulated wall-clock times for all tables are recorded again and the new data exchanges are executed within the next time-step.

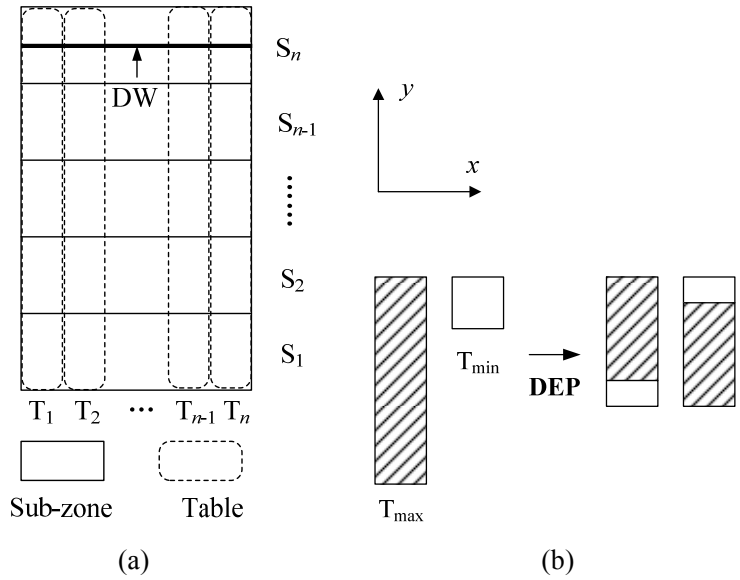

Fig. 1 The schematic of TP/DEP algorithm. (a) Transposed Processing (TP) strategy and (b) Data Exchange Processing (DEP) strategy. DW - detonation wave, S - sub-zone, T - table, subscript *n* is the number of tables (sub-zones), T_{max} – table with maximum operation time, T_{min} – table with minimum operation time.

A combination of TP strategy with DEP strategy is then applied into the numerical simulation of two-dimensionally gaseous detonation wave propagation, with the consideration of table size control method that is described in section 2.1. Compared to the algorithms based on the original

ISAT method proposed in ref. [24-28], the selected TP/DEP algorithm is obviously more suitable for the computations of transient, compressible, reacting flows with high Mach number in present study. The detailed comparison between present algorithm and those in ref. [24-28] is discussed in ref. [29].

3. Numerical Simulations of Gaseous Detonation

The propagation of gaseous detonation wave is one of typically compressible reacting flows, which is determined by its fine structures and interactions among these structures in spatial view and by quasi-periodical collision between triple points converged from the structures in temporal view. This spatio-temporal variations of detonation wave significantly affect the distribution of thermodynamic states in flow field and subsequently the table operations among data tables in corresponding sub-zones, when the parallel ISAT algorithm is adopted. Therefore, the numerical simulation of gaseous detonation is a suitable candidate to investigate the selected parallel algorithm with table size control mechanism for the purpose of chemistry acceleration computations.

3.1. Numerical model

The time-dependent, reactive, Euler equations in two-dimensional form are used to simulate the propagation process of a stoichiometric $2H_2+O_2$ detonation wave, which are expressed as:

$$\frac{\partial \mathbf{U}}{\partial t}+\frac{\partial \mathbf{F}}{\partial x}+\frac{\partial \mathbf{G}}{\partial y}=\mathbf{S} \tag{12}$$

where,

$$\mathbf{U}=\begin{pmatrix}\rho_1\\ \vdots\\ \rho_K\\ \rho u\\ \rho v\\ E\end{pmatrix},\quad \mathbf{F}=\begin{pmatrix}\rho_1 u\\ \vdots\\ \rho_K u\\ \rho u^2+p\\ \rho uv\\ u(p+E)\end{pmatrix},\quad \mathbf{G}=\begin{pmatrix}\rho_1 v\\ \vdots\\ \rho_K v\\ \rho uv\\ \rho v^2+p\\ v(p+E)\end{pmatrix},\quad \mathbf{S}=\begin{pmatrix}\dot{\omega}_1 W_1\\ \vdots\\ \dot{\omega}_K W_K\\ 0\\ 0\\ 0\end{pmatrix},$$

here, u, v are the velocity components in x and y spatial directions, respectively; p is the pressure, E represents the total energy of system; $\dot{\omega}_k$ is the net production rate of species k, W_k is the molecular weight of species k. The detailed interpretations of all these variables can be found in ref. [22].

The convection terms (**F** and **G**) in Eq. (12) are decoupled from the chemical reaction term (**S**) by using a splitting algorithm within each time-step. For the term **S**, we use a detailed H_2/O_2 mechanism [30] and employ the parallel acceleration algorithm with table size control method (see Sec. 2) to deal with it. For the purpose of comparisons, a DI (direct integration) method is also used to solve the term by using a VODE package [31]. To avoid unphysical oscillations and excessive

numerical dissipations in flow field, a Lax-Friedrichs (LF) flux splitting combined with a 9th-order WENO (weighted essentially non-oscillatory) scheme [32, 33] is employed to discretize the spatial derivatives of **F** and **G** in Eq. (12). The high-order and high-resolution simulations of the ninth-order WENO scheme has the advantages of flux smoothness and stability of the convergent solution, which is favorable at exhibiting the fragmentation of the fine structures in transient flow field for its small numerical dissipation [34, 35]. Lastly, the time derivative term in Eq. (12) is solved by a 3rd-order Runge-Kutta method with the constant time-step of 1.0×10^{-9}s. Note that the value of physical time-step for the splitting algorithm is obtained from CFL stability criterion. The value of 1.0×10^{-9}s is enough small to solve the stiff system in VODE computation and thus ensures that the use of splitting algorithm is reliable in present study.

3.2. Computational setups

The computational domain is a rectangle with $L_x\times L_y$ = 3mm×9mm, and is covered by square grids with size of $\Delta x=\Delta y$=0.01 mm, as shown in Fig. 2. The zero gradient condition is used for the top and bottom boundaries of the domain in y direction, while the left and right boundaries along x direction are the adiabatic slip rigid wall condition. The grid size (0.01mm) chosen in present study is the same as those in simulations of the same $2H_2+O_2$ detonations [36, 37]. This resolution had been demonstrated that the detonation cell size and structures are essentially independent of the computational grid size for the two-dimensional simulation [36, 37]. In addition, we adopt a moving computational domain along the direction of detonation wave propagation. Such motion of the domain ensures enough long distance for the propagation of detonation wave in y direction. For the purpose of parallel computations, the domain is divided into n sub-zones (S_1-S_n) with the same size along y direction and each processor is used in the corresponding sub-zone, as shown in Fig. 1(a).

Initially, a ZND detonation of $2H_2+O_2$ premixed gases is set within the region of y = 0-3 mm (see the gray part of the computational domain in Fig. 2), and the $2H_2+O_2$ premixed gases with initial temperature T_0=300K and initial pressure p_0=1atm are placed in the rest part of the domain. Moreover, a small disturbance area with high pressure of $38p_0$ is placed on the location just above the ZND region to form a cellular detonation quickly. Considering the non-physics of disturbance, only the results during the quasi-steady propagation of detonation wave (time-step=18,000-28,000) are collected and analyzed. During this period, the disturbance area has walked out the computational domain, and the detonation wave has been developed into a quasi-steady one with

the constant number of triple points. In addition, the number of sub-zones is set to n=15.

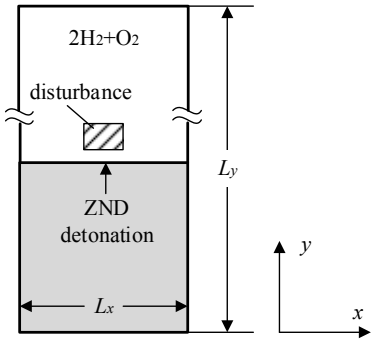

Fig. 2 Computational setups

3.3. Structure of cellular detonation

Figure 3 gives the structure of detonation wave computed by DI method at time-step=28,000 (quasi-steady state) in 15th sub-zone (S_{15}) which is located at the top of the computational domain. The cellular-like detonation wave front can be observed in this sub-zone, where the incident shock waves (SW), Mach stems (MS), transverse waves (TW) and triple points (TP) formed by these waves are clearly displayed in Fig. 3(a). The uneven distribution of the triple points along x direction is also found and thus suggests the non-uniform flow field. Figure 3(b) shows the mass fraction distribution of species H_2O_2, whose dark part represents the highly active reaction zone attached closely to the wave front.

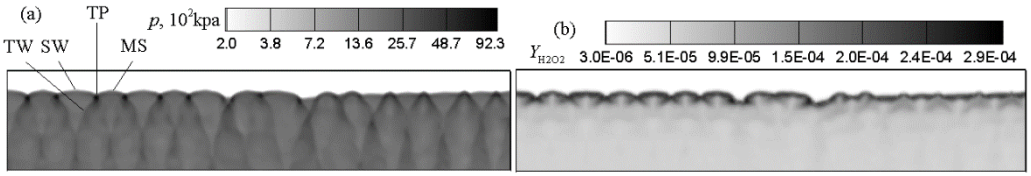

(a) (b)

Fig. 3 Structures of $2H_2+O_2$ detonation wave in the top sub-zone of computational domain, time-step=28,000. (a) pressure distribution, (b) mass fraction distribution of H_2O_2. SW – incident shock wave, MS – Mach stem, TW – transverse wave, TP – triple point.

Considering the numerical instability caused by the small numerical dissipation of the 9th-order WENO scheme [33], the shape of the reaction zone is randomly sinuous and thus presents as a thin layer along detonation wave front in Fig. 3(b). This indicates that the distribution of the thermodynamic states in the non-smooth region (wave front) is complicated due to the unsteady feature of the flow field, which can cause the difference among table operations and account for the necessity of the DEP strategy in present study. During the quasi-steady stage of computation for

gaseous detonation wave propagation, the averaged detonation velocity is 2819.96m/s, which is very close to the theoretical C-J detonation velocity (2843.16m/s) at the same physical conditions. Such good agreement between computational and theoretical values suggests the reliability of numerical simulations in present study. In addition, the constant of 14 triple points distributed on the wave front are found during the quasi-steady process.

4. Results and Discussions

In this section, we firstly analyze the computational efficiency of the selected TP/DEP algorithm with our novel table size control strategy. Tables 1 and 2 list the computational cases with different table sizes of total table control and the single table control, respectively. For all of cases, a fixed error tolerance with $\varepsilon_{tol}=1.0\times10^{-3}$ is set, and the number of tables (or sub-zones) is n=15. After then, the equilibrium and synchronization among the table operations are analyzed to explain the difference of acceleration effect among the cases in both Tables 1 and 2. The computational accuracies of the typical cases in present study are then examined in the last part of this section.

Table 1 Computational cases for total table size control with $M_{tot}=45.0\times10^6$

case	1	2	3	4	5
M_{sin} ($\times10^6$)	3.0	6.0	9.0	12.0	15.0

Table 2 Computational cases for single table size control with $M_{sin}=9.0\times10^6$

case	6	7	8	9	10	11	12
M_{tot} ($\times10^6$)	27.0	45.0	63.0	72.0	81.0	90.0	99.0

4.1. Efficiency analysis

Since the wall-clock time is the standard for evaluating computational efficiency of the chemical acceleration algorithm, thus we adopt a speedup ratio, R_s, to describe the computational efficiency, which is defined as the ratio of wall-clock time cost by DI to that cost by the parallel acceleration algorithm of TP/DEP.

The speedup ratios of all cases of $2H_2+O_2$ detonation in Tables 1 and 2 at time-step=28,000 are shown in Fig. 4. For total table size control cases with fixed $M_{tot}=45.0\times10^6$ in Fig. 4(a), R_s of each case in Table 1 is larger than 3.00 and a maximum one (4.29) can be achieved when $M_{sin}=9.0\times10^6$. On the other hand, for the single table size control cases with fixed $M_{sin}=9.0\times10^6$ in Fig. 4(b) and Table 2, a maximum R_s of 5.52 is obtained for case of $M_{tot}=63.0\times10^6$. Obviously, either single size or total size of all tables has the influence on the acceleration performance of parallel algorithm. For the fixed M_{tot}, increasing the M_{sin} can add more nodes in the table and consequently raise the retrieval

probability of nodes, but further increasing the M_{sin} may lead to premature deletion events for tables because the condition of fixed M_{tot} is met earlier. Therefore, larger M_{sin} leads to the decrease of R_s as shown in Fig. 4(a). For the fixed M_{sin} cases as shown in Fig. 4(b), larger M_{tot} provides larger memory space and is more beneficial for higher R_s. However, if M_{tot} continuously increases, part of tables can reaches the M_{sin} but another part cannot. This means that deletion events in all tables are occurred asynchronously and large amount of times are wasted on waiting for each other. Thus, there is a stage of decrease on R_s after $M_{tot}=63.0\times10^6$ in Fig. 4(b). At last, further increasing M_{tot} can give rise to the re-growth of R_s because the very large M_{tot} provides the environment with large memory in which almost all table can satisfy M_{sin} and the table operations can keep equilibrium. On the whole, the changing range of R_s at time-step=28,000 in cases listed in Table 2 is larger than that listed in Table 1, while the changing rule of curves in Figs. 4(a) and 4(b) are similar to each other. Thus, there is certainly an interaction between M_{sin} and M_{tot}, which further influence the speedup performance of the algorithm.

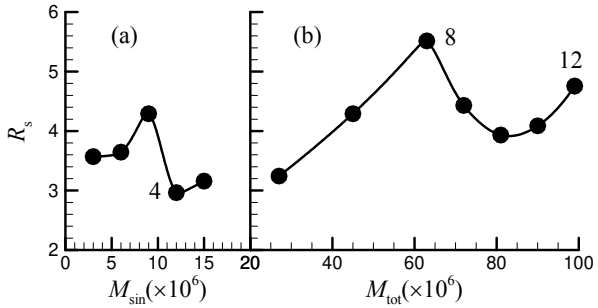

Fig. 4 The speedup ratios of the selected TP/DEP algorithm with table size control method at time-step=28,000 for cases of $2H_2+O_2$ detonation. (a) Cases based on the total table size control, (b) cases based on the single table size control. The numbers in the figure correspond to the cases in Tables 1 and 2.

Figure 5 gives the curves of R_s of three typical cases of $2H_2+O_2$ detonation (cases 4, 8 and 12) during the stable propagation process of detonation wave (time-step=18,000-28,000). Here, case 4 and case 8 correspond the computations with minimum and maximum R_s at time-step=28,000, respectively, while case 12 corresponds that with maximum total table size ($M_{tot}=99.0\times10^6$), as shown in Fig. 4. It can be observed that R_s for cases 4 and 12 undergoes a rapid raise at the initial time-steps followed by the decline to the relatively stable status. However, the R_s for case 8 displays the different variation from those for cases 4 and 12. In case 8, the R_s can continuously rise and reach a maximum value (10.6) at time-step=24,000 and then slowly decreases to the relatively stable

status.

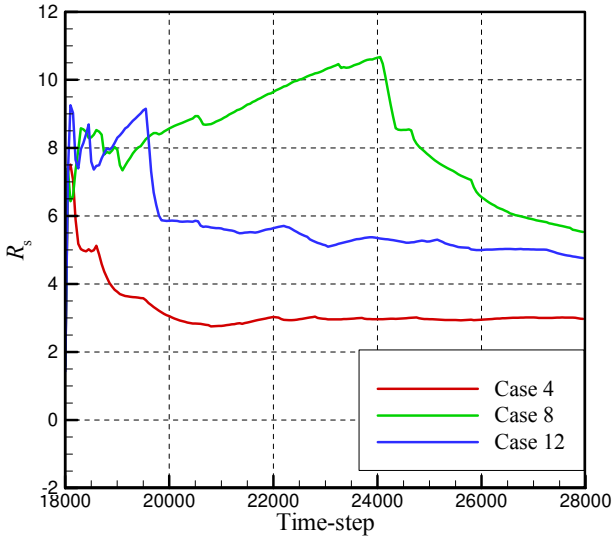

Fig. 5 Time histories of speedup ratios for typical cases of $2H_2+O_2$ detonation (time-step = 18,000-28,000).

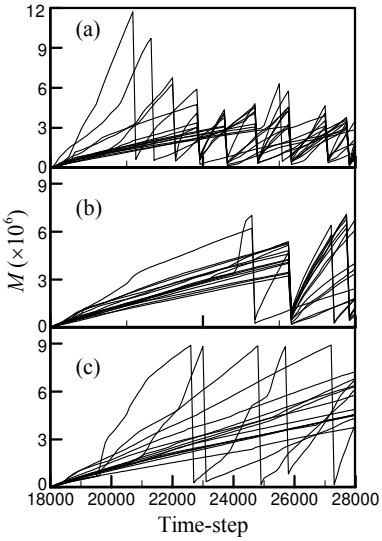

Fig. 6 The growth/reduction processes of all tables for the TP/DEP algorithm with table size control method in (a) case 4, (b) case 8 and (c) case 12.

To further interpret the difference of speedup performance among three cases, Fig. 6 gives the growth/deletion events of all tables for these cases. On the whole, the growth/deletion processes of tables for these cases are different from each other. In Fig. 6(a), case 4 corresponds to the total size control of all tables. Since the sum of each single table size here is $n\times M_{sin}=15\times12.0\times10^6=180.0\times10^6$ that is much larger than $M_{tot}=45.0\times10^6$, the nodal deletion is always determined by the M_{tot} and is performed for most of tables in which the node number does not reaches their M_{sin} (12.0×10^6). Thus, growth/deletion events occur frequently and consequently lead to the low R_s (3.00) at time-step=28,000, as seen in Fig. 4(a). Note that synchronous deletion/growth behavior can be observed for most of tables and implies the synchronization of table operations among the tables. For another typical case (case 8 of Fig. 6b), the obvious reduction of deletion/growth events in most tables is observed and the synchronization among the tables is also good. Therefore, case 8 gets the highest R_s for all cases in Figs. 4 and 5, due to improvements of both growth/deletion frequency and synchronization. Figure 6(c) shows the last typical case in which the nodal deletion is always determined by the M_{sin} due to the largest M_{tot}. In this case, the deletion/growth events are relatively less but the synchronization is poor. Higher R_s (4.76 at time-step=28,000) in case 12 implies that reduction of the deletion/growth events of the tables dominates the acceleration performance of the parallel algorithm.

4.2. Equilibrium and synchronization analyses

The above results show that the acceleration performance of the algorithm is dependent on the deletion/growth events and the synchronization of the table operations. In this section, we define a standard deviation, σ_f, of frequency of deletion/growth events to characterize the equilibrium of table operations among the tables, which is expressed as

$$\sigma_f = \left(\frac{1}{n} \sum_{i=1}^{n} \left(f_i - \overline{f} \right)^2 \right)^{1/2} \tag{13}$$

here f_i is the deletion/growth frequency of the i-th table, which means the number of deletion events in this data table during the entire computation of quasi-state propagation of detonation wave, $\overline{f}$ is the mean value of f_i for all of tables in the whole computational domain, n is the number of tables. Furthermore, we introduce a parameter p to describe the synchronization among the table operations, which is given by

$$p = \frac{t_w}{\overline{t_c}} \tag{14}$$

here, t_w and $\overline{t_c}$ represent the actual wall-clock time cost in the chemical reactions and the averaged one of accumulated CPU time of all data tables by time-step=28,000, respectively. One extreme case of p is that the synchronization is best when p=1, suggesting the actual wall-clock time is completely determined by the averaged accumulated CPU time of table operations. The larger the p is, the worse the synchronization is.

Figures 7(a) and 7(b) present the correlations between R_s and σ_f and between R_s and p for all cases of $2H_2$+O_2 detonation in Tables 1 and 2. It can be seen from Fig. 7(a) that good correlation with correlated coefficient R^2=0.7835 between R_s and σ_f can be obtained, and that the smaller σ_f corresponds to the higher R_s. The result suggests that the equilibrium denoted by σ_f has important influence on the computational efficiency, which is totally consistent with that shown in Figs. 5 and 6. The result in Fig. 7(b) shows the poor correlation between R_s and p for all cases. However, if we remove the cases 9-12 with large M_{tot} ($\geq 72.0\times10^6$, see Table 2), the good correlation is still obtained with R^2=0.8081. Such result reveals that good synchronization (small p) is beneficial to improvement of the acceleration performance (large R_s), provided that total size of tables is not excessively large.

Furthermore, a mixed index of p and σ_f, $(p\times\sigma_f)^{1/2}$, is defined to represent the combined effect of equilibrium and synchronization among table operations. The correlation between R_s and $(p\times\sigma_f)^{1/2}$

is shown in Fig. 7(c). This result is similar to that shown in Fig. 7(a), which indicates the strong effect of the equilibrium on the speedup ratio. On the other hand, the synchronization index of p exhibits the indirect influence to the acceleration performance in all cases (including the cases 9-12 with large M_{tot}) through the combination to σ_f, which is different from that in Fig. 7(b).

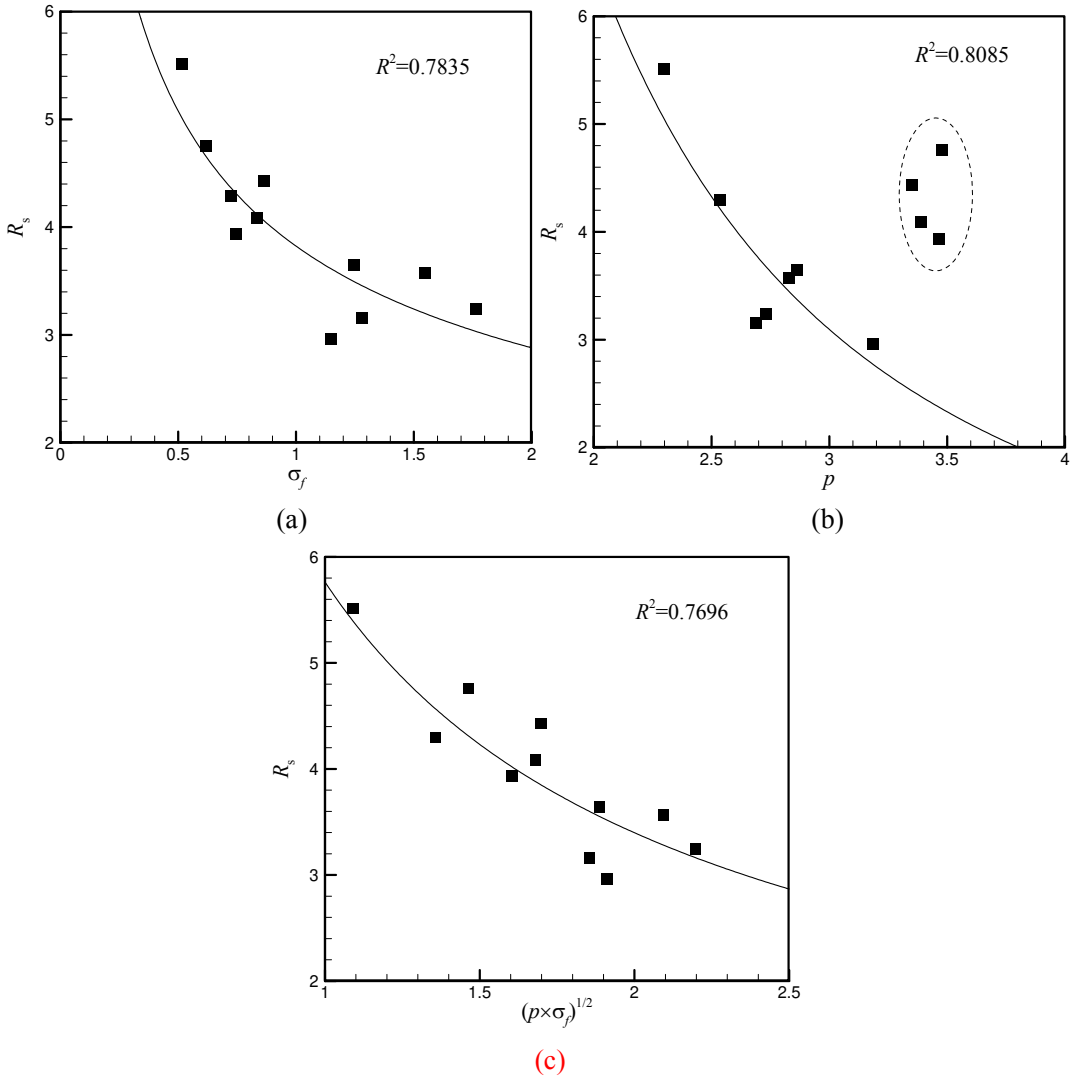

Fig. 7 Correlation between (a) σ_f and R_s, (b) p and R_s and (c) $(p\times\sigma_f)^{1/2}$ and R_s for $2H_2+O_2$ detonation cases. The data within the dashed ellipsoid correspond to the cases 9-12 in Table 2.

Although the results in Fig. 7 show that both equilibrium and synchronization among table operations play the important roles together in the computations, there is no explicit indicator to help user to conveniently determine the suitable table size with the given computer memory. Thus, we define a parameter, p_M, which represents the ratio between theoretical upper limit and realistic upper limit of node numbers, to help users for choosing the most suitable table sizes (including M_{sin} and M_{tot}). This parameter is expressed as follows.

$$p_{\mathrm{M}} = \frac{n \times M_{\mathrm{sin}}}{M_{\mathrm{tot}}} \tag{15}$$

The square symbols in Fig. 8 shows the relationship between R_s and p_M for all computational cases of $2H_2+O_2$ detonation. These results indicate that cases with higher speedup ratios are mostly appears when the range of p_M is about 1.3-2.2. This range means the great equilibrium and synchronization among table operations (e.g., cases 8 and 12 as shown in Figs. 4 and 5). Usually, the computer total memory and the number of sub-zones n in parallel computations are both known in advance by users. Thus, we can firstly determine total table size M_{tot} based on the computer total memory to make full use of the memory space, and then obtain the suitable single table size M_{sin} by Eq. (15) within an optimal range of 1.3-2.2.

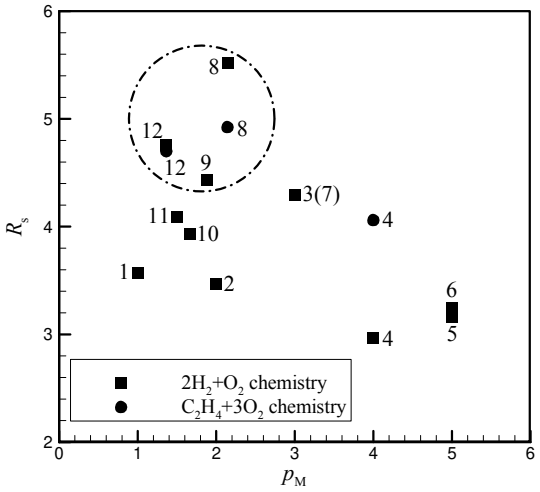

Fig. 8 Relationship between p_M and R_s for cases of different fuels detonations. The cases within the dashed circle represent those with higher R_s.

The rationality of the optimal p_M range should be verified in other simulations with different computational conditions (e.g. different fuel types). Since the $2H_2+O_2$ detonation is considered to be a reacting flow with a small chemistry, a propagation process of a stoichiometric $C_2H_4+3O_2$ detonation wave with relatively large reaction mechanism of ethylene/oxygen [38] are numerically simulated to identify the optimal p_M range (1.3-2.2). For the simulations of $C_2H_4+3O_2$ detonation, the physical and numerical conditions are the same as those for the $2H_2+O_2$ detonations, see Secs. 3.1 and 3.2. Also, the data with 10,000 time-steps (12,100-22,100) for quasi-steady propagation of detonation wave are computed and collected. The simulations of three typical cases which also correspond to cases 4, 8 and 12 in Tables 1 and 2, are carried out by using our parallel algorithm with table size control strategy. At the last time-step, the speedup ratios of three cases (4, 8 and 12) for $C_2H_4+3O_2$ detonations are 4.06, 4.92 and 4.70, respectively. The relationship between p_M and R_s

for these cases is also depicted in Fig. 8. It can be seen that the R_s of three typical cases with ethylene chemistry shows the similar distribution with that of those cases with hydrogen chemistry. The higher speedup ratios for cases 8 and 12 still fall into the optimal range of p_M (p_M=2.1 and 1.4 for both cases), while relatively lower speedup ratio for case 4 is out of the range (p_M=4.0). Such results indicate that the acceleration performance of our parallel algorithm with table size control strategy is stable for different chemical reaction mechanisms, and that optimal p_M is also insensitive to the fuel type for detonation simulations.

4.3. Accuracy analysis

In order to examine the computational accuracy of the parallel algorithm with table size control strategy, we firstly give the relative errors of the mean propagation velocity of detonation wave to theoretical C-J detonation wave velocity during the whole quasi-steady propagation process for selected cases 4, 8 and 12. Figure 9 shows these relative errors of three cases for both $2H_2+O_2$ detonation and $C_2H_4+3O_2$ detonation. It can be seen from Fig. 9(a) that all relative errors in $2H_2+O_2$ detonation are within ±0.5%, while all relative errors in $C_2H_4+3O_2$ detonation in Fig. 9(b) are also no more than 0.8%. Therefore, the computational accuracy of our parallel algorithm with table size control strategy is examined to be reliable.

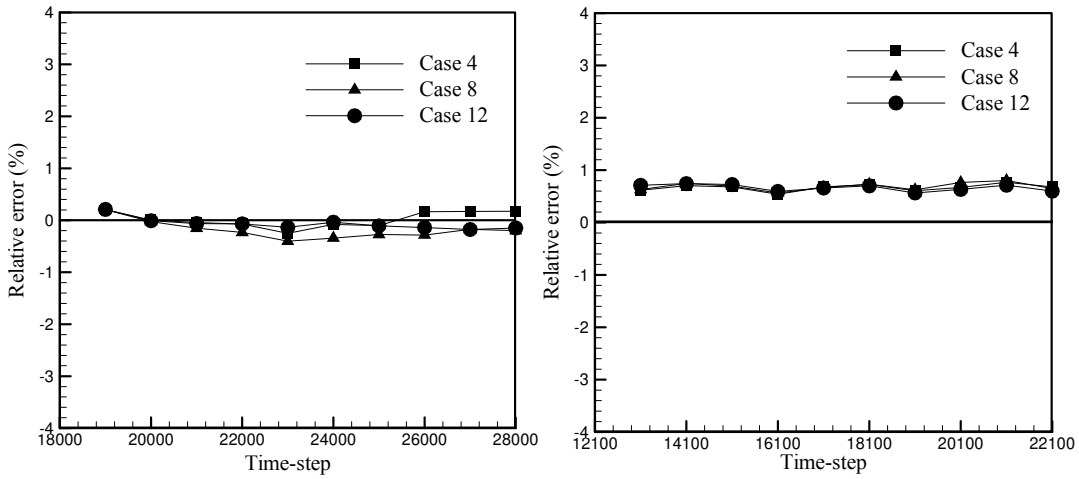

(a) (b)

Fig. 9 The relative errors between the mean propagation velocity of detonation wave to the theoretical C-J value by the TP/DEP algorithm with table size control strategy for different cases in (a) $2H_2+O_2$ detonation during time-step = 18,000-28,000 and (b) $C_2H_4+3O_2$ detonation during time-step = 12,100-22,100.

Typically, we also give the instantaneous distributions of the spatial-averaged form of the solutions in flow field for selected three cases (cases 4, 8 and 12) of $2H_2+O_2$ detonation. The

solutions by the algorithm with table size control strategy are then compared with those by the DI method. The averaged form of the solutions is expressed as

$$\bar{U}(y,t)=\frac{1}{L_x}\int_0^{L_x}U(x,y,t)\mathrm{d}x \tag{16}$$

here, $U(x, y, t)$ represents the instantaneous solutions at the position (x, y) of flow field at moment t, L_x is the transverse length of computational domain in x direction. Thus, the $\bar{U}(y,t)$ represents the spatial-averaged solutions along the y direction (i.e., the direction of detonation wave motion).

Figure 10 gives the profiles of spatial-averaged pressure, temperature, mass fraction of OH and mass fraction of H_2O_2 computed by Eq. (16) for cases 4, 8 and 12 of $2H_2+O_2$ detonation at time-step = 28,000. These results are compared with those obtained by DI at the same moment. It is found that the profiles of three typical cases by our parallel algorithm with table size control are all well consistent with those obtained by DI method, which again proves the good accuracy of the algorithm. In addition, there is no significant difference among the profiles of these cases in Fig. 10, indicating that the accuracies for all cases are independent on the table size control of the parallel acceleration algorithm.

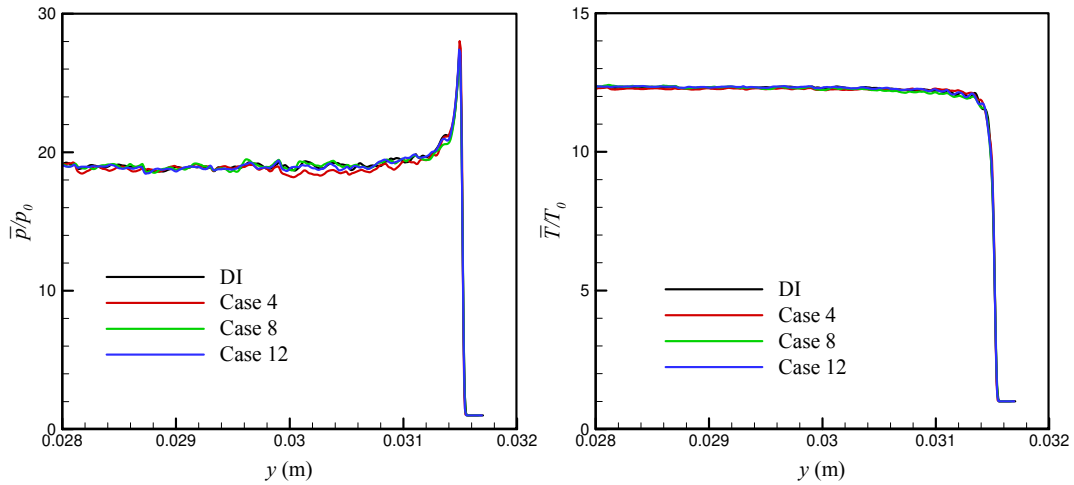

(a) (b)

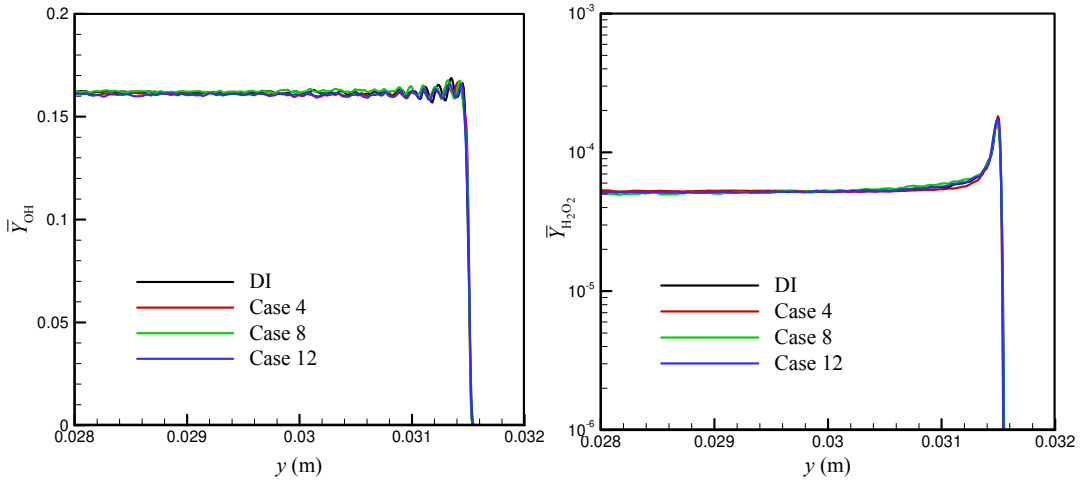

(c) (d)

Fig. 10 Distributions of integrated quantities by the DI method and the TP/DEP algorithm with table size control method for different cases at time-step = 28,000 for $2H_2+O_2$ detonation. (a) pressure, (b) temperature, (c) mass fractions of OH, (d) mass fractions of H_2O_2.

5. Concluding Remarks

For the purpose of chemistry acceleration in the parallel computations of transient, compressible and reacting flows, a size control strategy of data tables, which includes the single table size control method and the total table size control method, is proposed and combined with a selected parallel TP/DEP algorithm that is based on the reduced ISAT technique. The combined algorithm is then applied to the numerical simulations of two-dimensionally gaseous detonation wave propagation, to examine both of computational efficiency and accuracy.

The results of computational efficiency show that the speedup ratios of the algorithm vary with the changes of single table size and/or total table size. For all cases of $2H_2+O_2$ detonation in present study, a maximum speedup ratio of R_s =5.52 and a minimum speedup ratio of R_s =3.00 can be obtained in the end of computations. While for selected cases of the $C_2H_4+3O_2$ detonation, the speedup ratio ranged in 4.06-4.92 is achieved. All results in present study show the effectiveness on chemically acceleration computations. Two concepts, that is, equilibrium and synchronization, are introduced to analyze the effects of single table size control and total table size control on the speedup performance of our parallel algorithm. The correlation analyses show that both equilibrium and synchronization have the obvious influences on computational efficiency. The improvements on equilibrium and synchronization of table operations among different ISAT tables mapped into corresponding sub-zones in the whole computational domain are in favor of the enhancement of the computational efficiency. In addition, a parameter that helps users choose the suitable table sizes is

proposed to achieve better speedup ratio of the algorithm. This parameter shows an optimal range that is favor of the chemistry acceleration of detonation simulations, either in small hydrogen chemistry or in relatively large ethylene chemistry.

Lastly, the computational accuracy of results in all selected typical cases obtained by the parallel algorithm with table size control strategy are examined to be reliable for both $2H_2+O_2$ and $C_2H_4+3O_2$ detonations.

Acknowledgement

The authors gratefully acknowledge the support of the Natural Scientific Foundation of China (NSFC) under grant No. 11872213. The authors sincerely appreciate the reviewers and editors for their valuable comments.

References

[1] Warnatz J., Mass U., Dibble R. W. Combustion: physical and chemical fundamentals, modelling and simulation, experiments, pollutant formation, Springer, Berlin (2006) (4th Edition) https://doi.org/10.1007/978-3-540-45363-5

[2] Chen J. Y., Kollmann W., Dibble R. W. PDF modeling of turbulent non-premixed methane jet flames, *Combustion Science and Technology*, **64**(4-6), 315-346 (1989) https://doi.org/10.1080/00102208908924038

[3] Turányi T. Parameterization of reaction mechanisms using orthonormal polynomials, *Computers and Chemistry*, **18**(1), 45-54 (1994) http://dx.doi.org/10.1016/0097-8485(94)80022-7

[4] Christo F. C., Masri A. R., Nebot E. M. Artificial neural network implementation of chemistry with PDF simulation of H_2/CO_2 flames, *Combustion and Flame*, **106**(4), 406-427 (1996) http://dx.doi.org/10.1016/0010-2180(95)00250-2

[5] Blasco J. A., Fueyo N., Dopazo C., et al. Modelling the temporal evolution of a reduced combustion chemical system with an artificial neural network, *Combustion and Flame*, **113**(1–2), 38-52 (1998) http://dx.doi.org/10.1016/S0010-2180(97)00211-3

[6] Pope S. B. Computationally efficient implementation of combustion chemistry using in *situ* adaptive tabulation, *Combustion Theory and Modelling*, **1**(1), 41-63 (1997) https://doi.org/10.1080/713665229

[7] Rabitz H., Aliş F. Ömer. General foundations of high-dimensional model representations, *Journal of Mathematical Chemistry*, **25**(2-3), 197-233 (1999) https://doi.org/10.1023/A:1019188517934

[8] Tonse S. R., Moriarty N. W., Brown N. J., et al. PRISM: piecewise reusable implementation of solution mapping. An economical strategy for chemical kinetics, *Israel Journal of Chemistry*, **39**(1), 97–106 (1999) http://dx.doi.org/10.1002/ijch.199900010

[9] Bell J. B., Brown N. J., Day M. S., et al. Scaling and efficiency of prism in adaptive simulations of turbulent premixed flames , *Proceedings of the Combustion Institute*, **28**(1), 107-113 (2000) http://dx.doi.org/10.1016/S0082-0784(00)80201-5

[10] Xu J., Pope S. B. PDF calculations of turbulent non-premixed flames with local extinction, *Combustion and Flame*, **123**(3), 281-307 (2000) http://dx.doi.org/10.1016/S0010-2180(00)00155-3

[11] Tang Q., Xu J., Pope S. B. Probability density function calculations of local extinction and no production in piloted-jet turbulent methane/air flames, *Proceedings of the Combustion Institute*, **28**(1), 133-139 (2000) http://dx.doi.org/10.1016/S0082-0784(00)80204-0

[12] Cao R. R., Pope S. B. The influence of chemical mechanisms on PDF calculations of non-premixed piloted jet flames, *Combustion and Flame*, **143**(4), 450-470 (2005) http://dx.doi.org/10.1016/j.combustflame.2005.08.018

[13] Liu B. J. D., Pope S. B. The performance of in *situ* adaptive tabulation in computations of turbulent flames, *Combustion Theory and Modelling*, **9**(4), 549-568 (2005) https://doi.org/10.1080/13647830500307436

[14] Gordon R. L., Masri A. R., Pope S. B., et al. A numerical study of auto-ignition in turbulent lifted flames issuing into a vitiated co-flow, *Combustion Theory and Modelling*, **11**(3), 351-376 (2007) http://dx.doi.org/10.1080/13647830600903472

[15] Fooladgar E., Chan C. K., Nogenmyr K. J. An Accelerated Computation of Combustion with Finite-rate Chemistry using LES and an Open Source Library for In-Situ-Adaptive Tabulation. *Computers and Fluids*, **146**, 42-50 (2017) http://dx.doi.org/10.1016/j.compfluid.2017.01.008

[16] Avdić A., Kuenne G., Mare F. D., et al. LES combustion modeling using the Eulerian stochastic field method coupled with tabulated chemistry. *Combustion and Flame*, **175**, 201-219 (2016) https://doi.org/10.1016/j.combustflame.2016.06.015

[17] Liang Y., Pope S. B., Pepiot P. A pre-partitioned adaptive chemistry methodology for the efficient implementation of combustion chemistry in particle PDF methods. *Combustion and Flame*, **162**(9), 3236-3253 (2015) https://doi.org/10.1016/j.combustflame.2015.05.012

[18] Contino F., Jeanmart H., Lucchini T., et al. Coupling of in *situ* adaptive tabulation and dynamic adaptive chemistry: An effective method for solving combustion in engine simulations, *Proceedings of the Combustion Institute*, **33**(2), 3057-3064 (2011) http://dx.doi.org/10.1016/j.proci.2010.08.002

[19] Yang B., Pope S. B. Treating chemistry in combustion with detailed mechanisms-In *situ* adaptive tabulation in principal directions-Premixed combustion, *Combustion and Flame*, **112**(1-2), 85-112 (1998) http://dx.doi.org/10.1016/S0010-2180(97)81759-2

[20] Ren Z., Liu Y., Lu T., et al. The use of dynamic adaptive chemistry and tabulation in reactive flow simulations, *Combustion and Flame*, **161**(1), 127-137 (2014) http://dx.doi.org/10.1016/j.combustflame.2013.08.018

[21] Kumar A., Mazumder S., Adaptation and application of the In *Situ* Adaptive Tabulation (ISAT) procedure to reacting flow calculations with complex surface chemistry, *Computers and Chemical Engineering*, **35**(7), 1317-1327 (2011) http://dx.doi.org/10.1016/j.compchemeng.2010.10.005

[22] Dong G., Fan B. C., Chen Y. L. Acceleration of chemistry computations in two-dimensional detonation induced by shock focusing using reduced ISAT, *Combustion Theory and Modeling*, **11**(5), 823-837 (2007) http://dx.doi.org/10.1080/13647830701316657

[23] Dong G., Fan B. C. Chemistry acceleration modeling of detonation based on the dynamical storage/deletion algorithm, *Combustion Science and Technology*, **181**(9), 1207-1216 (2009) http://dx.doi.org/10.1080/00102200903181744

[24] Lu L., Lantz S. R., Ren Z., et al. Computationally efficient implementation of combustion chemistry in parallel PDF calculations, *Journal of Computational Physics*, **228**(15), 5490-5525 (2009) http://dx.doi.org/10.1016/j.jcp.2009.04.037

[25] Lu L., Ren Z., Lantz S. R., et al. Investigation of strategies for the parallel implementation of ISAT in LES/FDF/ISAT computations, in: Fourth Joint Meeting of the US Sections of the Combustion Institute, Drexel University, Philadelphia, PA, 20-23 March (2005)

[26] Hiremath V., Lantz S. R., Wang H., et al. Computationally-efficient and scalable parallel implementation of chemistry in simulations of turbulent combustion, *Combustion and Flame*, **159**(10), 3096–3109 (2012) http://dx.doi.org/10.1016/j.combustflame.2012.04.013

[27] Hiremath V., Lantz S. R., Wang H., et al. Large-scale parallel simulations of turbulent combustion using combined dimension reduction and tabulation of chemistry, *Proceedings of the Combustion Institute*, **34**(1), 205-215 (2013) http://dx.doi.org/10.1016/j.proci.2012.06.004

[28] Heye C., Raman V., Masri A. R. Influence of spray/combustion interactions on auto-ignition of methanol spray flames, *Proceedings of the Combustion Institute*, **35**(2), 1639-1648 (2015) http://dx.doi.org/10.1016/j.proci.2014.06.087

[29] Wu J. T., Dong G., Li B. M. Parallel chemistry acceleration algorithms based on ISAT method in gaseous detonation computations, *Computers and Fluids*, **167**, 265-284 (2018) http://dx.doi.org/10.1016/j.compfluid.2018.03.036

[30] Burke M. P., Chaos M., Ju Y., et al. Comprehensive H_2/O_2 kinetic model for high - pressure combustion. *International Journal of Chemical Kinetics*, **44**(7), 444-474 (2012) http://dx.doi.org/10.1002/kin.20603

[31] Brown P. N., Byrne G. D., Hindmarsh A. C. VODE: a variable-coefficient ODE solver. *Society for Industrial and Applied Mathematics*, **10**(5), 1038-1051 (1989) http://dx.doi.org/10.1137/0910062

[32] Jiang G. S., Shu C. W. Efficient implementation of weighted ENO schemes. *Journal of Computational Physics*, **126**(1), 202-228 (1996) http://dx.doi.org/10.1006/jcph.1996.0130

[33] Balsara D. S., Shu C. W. Monotonicity preserving weighted essentially non-oscillatory schemes with increasingly high order of accuracy, *Journal of Computational Physics*, **160**(2), 405-452 (2000) http://dx.doi.org/10.1006/jcph.2000.6443

[34] Latini M., Schilling O., Don W. S. Effects of WENO flux reconstruction order and spatial resolution on re-shocked two-dimensional Richtmyer-Meshkov instability. *Journal of Computational Physics*, **221**(2), 805–836 (2007) http://dx.doi.org/10.1016/j.jcp.2006.06.051

[35] Zhang Y. T., Shi J., Shu, C. W., et al. Numerical viscosity and resolution of high-order weighted essentially non-oscillatory schemes for compressible flows with high Reynolds numbers. *Physical Review E Statistical Nonlinear and Soft Matter Physics*, **68**, 046709 (2003) https://doi.org/10.1103/PhysRevE.68.046709

[36] Gamezo V. N., Desbordes D., Oran E. S. Formation and evolution of two-dimensional cellular detonations. *Combustion and Flame*, **116**(1–2), 154-165 (1999) http://dx.doi.org/10.1016/S0010-2180(98)00031-5

[37] Gamezo V. N., Desbordes D., Oran E. S. Two-dimensional reactive flow dynamics in cellular detonation waves. *Shock Waves*, **9**(1), 11-17 (1999) http://dx.doi.org/10.1007/s001930050134

[38] G. Dong, B. C. Fan, J. F. Ye, Numerical investigation of ethylene flame bubble instability induced by shock waves, Shock Waves 17(6) (2008) 409-419. http://dx.doi.org/10.1007/s00193-008-0124-3